Micromagnetic modeling of the polycrystalline structure effect to the hysteresis loop in ferromagnetic nanowire

Micromagnetic modeling of the polycrystalline structure effect to the hysteresis loop in ferromagnetic nanowire

S A Satsuk and S V Komogortsev

Kirensky Institute of Physics, Federal Research Center KSC SB RAS, 50 Akademgorodok, 660036 Krasnoyarsk, Russia

E-mail: svetlana.satsuk@gmail.com

Abstract. Extensive micromagnetic simulation results of the hysteresis loops in ferromagnetic nanowire with randomly oriented crystallites ordered in one chain is presented. Three main contributions to the magnetic energy of the wire had been taken into account: exchange, dipole-dipole, and the magnetic anisotropy energy of the crystallite. In cases where one of the three contributions to the energy can be neglected, the numerical calculations are in good agreement with the results of the well-known, analytically studied micromagnetic problems. In the case when all three contributions are comparable, a complex non-monotonic dependence of the coercive force on the crystallite size and the magnetic anisotropy constant is observed. In order to interpret these changes, a new micromagnetic scale is introduced, which takes into account all three contributions to the magnetic energy of the wire, and performs a correct transition to the analytically studied limits, which take into account the competition of any two contributions.

1. Introduction

The study of the magnetic properties of nanowires (NW), which started several decades ago, is a rapidly developing area due to the latest achievements in theory, synthesis technology and the development of experimental research methods [1–4]. The transverse size of nanowires varies from units to hundreds of nanometers, while its length exceeds the transverse size by at least an order of magnitude. Nanowires are promising candidates for the creation of composite matrices used in storage and recording systems, various sensors and other devices with unique properties [5–8]. The specific applications of the functional magnetic element are determined by the magnetic hysteresis loop. For nanoelements with a large aspect ratio, pronounced difference in hysteresis magnetic properties is observed in comparison with macroscopic analog materials. One of the most important reasons for this difference is that the size of the functional element is comparable to the characteristic micromagnetic sizes (the correlation length of the exchange interaction, the width of the domain wall, etc.) [9, 10].

At present, a significant amount of information has been accumulated on the nature of the magnetization reversal processes in nanowires, including precisely solvable micromagnetic problems, numerical simulation, and experimental studies [4, 9, 11–14]. Note that the understanding of magnetic hysteresis in nanowires is limited by several simplified analytical models, such as the coherent rotation model [15], the curling model [16, 17], and the activation volume model [11, 18]. Micromagnetic modeling allows calculating the hysteresis loop by numerically solving the Landau-Livshitz equation and achieving satisfactory agreement for a certain set of micromagnetic constants [10]. This possibility undoubtedly enhances our understanding, but it is necessary to conduct a systematic study of the

relationship between the shape, size, micromagnetic constants, and structure of wire with magnetic hysteresis. In particular, a study of the structure of the nanowires prepared by the well-known methods of template synthesis shows that they have a polycrystalline structure [19–23]. The effect of the polycrystalline structure on hysteresis is primarily associated with disorder in the direction of the easy magnetization axes of individual crystallites. This disorder is taken into account in the so-called models of random magnetic anisotropy (RMA) [24], along with the exchange interaction between neighboring crystallites. Unfortunately, the analytical consideration of the dipole-dipole interaction significantly complicates the problem, so that analytical results can be obtained only for a very narrow class of approximations [14].

The present work is devoted to a numerical study of the effect of the polycrystalline structure of a ferromagnetic nanowire on their coercive force by the method of micromagnetic simulation. Systematic numerical research is a very complex problem. Besides the different ratios of three energies (anisotropy energy, exchange energy, energy of dipole-dipole interaction), different dimensions of the correlation volumes of the magnetic microstructure are possible here: from one-dimensional (one crystallite in the cross-section of a nanowire) [25] to three-dimensional (the crystallite size is much smaller than the cross-section of a nanowire) [18, 21]. Here we will consider only the one-dimensional case.

In this work, we attempt to systematically investigate the effect of the polycrystalline structure of a one-dimensional nanowire on its properties. In the numerical experiment, this feature was taken into account as follows: the magnetic nanowire is represented by a chain of exchange-coupled crystallites (cubic cells of size a, the length of the wire is much larger than the crystallite size (aspect ratio L/d is not less than 100). In order to take into account, the polycrystalline structure of the material, each cell of size a is considered as a separate crystallite. The saturation magnetizations and the magnetic anisotropy constants K of the cells are the same, and the easy magnetization axes of various crystallites are randomly oriented. In this system, complex inhomogeneous configurations of magnetization are realized, determined by the competition of three contributions to the total energy: exchange energy, magnetic dipole energy, and the energy of local magnetic anisotropy of the crystallite.

2. Numerical experiment and discussion

The calculation was performed using the object-oriented micromagnetic platform OOMMF [26]. Computer calculation of micromagnetic states and magnetization curves in the OOMMF package is based on the numerical solution of the Landau-Lifshitz equation by the finite difference method [27].

In calculations, a nanowire was considered as a one-dimensional chain of exchange-coupled crystallites; the type of nanowire material was specified by choosing an anisotropy constant and an exchange constant. The calculations were performed in a magnetic field oriented along the long axis of the nanowire. In this geometry, the demagnetizing factor is close to zero. Thus, the influence of the shape anisotropy is reduced here to an addition to the total energy, and the magnetization distribution corresponds to the simplest case, when the deviation of the magnetization from the direction of the external field is completely symmetric. For such a field direction, in limiting cases, there are analytical solutions that will serve as benchmarks for interpreting a numerical experiment. We calculated several series of loops (conventionally named as **A**, **B**, **C**, **D**) with different parameters of the micromagnetic problem (see table 1). For all numerical calculations, it was assumed that the cell size $a = 10\,nm$ is equal to the cross-sectional size d, the nanowire length is $L = 10^4 nm$, and the magnetization is $M_s = 1000\,G$.

*2.1 Series **A***

The first series of hysteresis loops was calculated for various values of the local magnetic anisotropy constant *K*, while the exchange constant *A* remained constant.

Table 1. Parameters of numerical experiments

Loop series	**A**	**B**	**C**	**D**
A (10^{-6} erg/cm)	1	0..4	0..4	0..4
K (10^6 erg/cm^3)	0..10	0.015	3	6.5

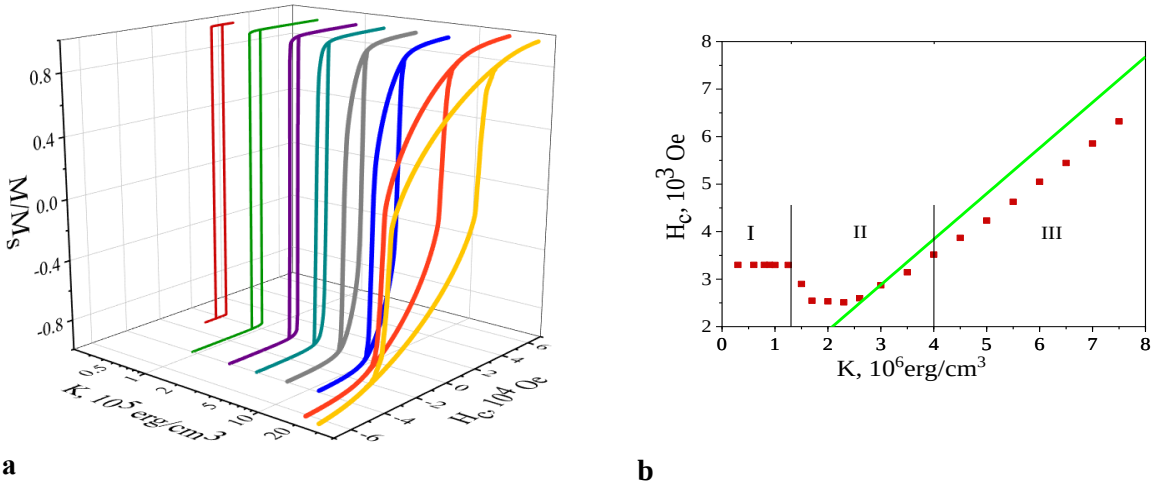

a **b**

Figure 1. a) Hysteresis loops for different values of the anisotropy constant. The calculation parameters are shown in table 1. b) Dependence of the coercive force on the anisotropy constant obtained from the corresponding hysteresis loops (figure 1 a). The figure shows three regions: I - region of weak anisotropy, II - region of medium anisotropy, III - region of strong anisotropy. The green line corresponds to the dependence of the coercive force on the anisotropy constant based on the Stoner-Wolfarth model $H_c = 0.48\frac{2K}{M_S}$.

The hysteresis loops (figure 1a) differ significantly for different K values. It is seen that with an increase of the anisotropy energy, the coercive field increases. At small values of the anisotropy constant, the loop is almost rectangular, while at large values it is rounded. The calculated hysteresis loops were used to calculate and plot the dependence of the coercive field H_c on the anisotropy constant (figure 1b). The obtained $H_c(K)$ curve allows to qualitatively distinguish three main modes.

When the anisotropy constant is significantly less than the energy of the dipole-dipole interaction ($E_d = \pi M_s^2 \approx 3.14 \cdot 10^6 erg/cm^3$) and exchange energy ($E_{ex} = 2A/a^2 \approx 2 \cdot 10^6 erg/cm^3$) it does not affect H_c, which is what we observe in the K range from 0 to $10^6 erg/cm^3$ (region I in figure 1.b).

When the local magnetic anisotropy is very strong (the magnetic anisotropy energy ($E_a \equiv K$) is higher than energy of dipole-dipole interaction energy E_d and exchange energy E_{ex}), the magnetic anisotropy constant K is the main factor determining the coercive force H_c. In this case, we observe a linear correlation between K and H_c (region III in figure1.b, where $K > 5 \cdot 10^6 erg/cm^3$).

In the intermediate value range $K = 10^6 \dots 5 \cdot 10^6 erg/cm^3$ a complex behavior of H_c is observed: instead of a gradual growth with increasing of K (see, for example [28]), the passage of a local minimum is reliably observed followed by the growth observed in mode III. This unusual behavior is related to the fact that in this range all three main contributions to the total energy (exchange, dipole-dipole, and anisotropy) are of the same order (region II in figure 1.b).

For the first case (region I), there are analytical solutions [15] corresponding to the Stoner-Wolfarth model, when the magnetization curve is determined only by the magnetic shape anisotropy. The third

case corresponds to the Stoner-Wolfarth model, when the magnetization curve is determined only by the magnetic anisotropy of randomly oriented crystallites. Here its influence on the coercive force can be calculated as: $H_c = 0.48\frac{2K}{M_S}$[15]. For region II there are no analytical solutions. Therefore, computer calculations are the only way to obtain information on the magnetic hysteresis in this range of magnetic anisotropy constants. Since in reality all three contributions to the total energy should be taken into account, we considered the magnetization reversal of the samples in each of the selected regions (I, II, and III).

*2.2 Series **B***

In this region the main competing contributions are the energy of the dipole-dipole interaction and the exchange energy. We changed the energy ratio by manipulating the values of the exchange constant (the ranges of A and the selected value of the anisotropy constant are given in table 1). Figure 2a shows the sequence of hysteresis loops for different A constants. Note that the ratio of competing energies can be unambiguously associated with the ratio of spatial scales $E_d/E_{ex} = (a/l_{ex})^2$, where $l_{ex} = \sqrt{\frac{A}{\pi {M_S}^2}}$. This feature allows you to track the H_c dependence on the reduced crystallite size, which is important from the point of view of experimental analysis and synthesis of new materials. Therefore, in figure 2b we present the dependences of the coercive force on the ratio of scales a/l_{ex}. The value of H_c here is limited by the magnetic shape anisotropy field $H_{sh} = 2\pi M_S$, therefore, figure 2b shows the reduced coercive force H_c/H_{sh}. Extrapolation of a/l_{ex} to zero corresponding to the overwhelming contribution of the exchange interaction leads to $\frac{H_c}{H_{sh}} = 1$, i.e. to the equality $H_c = H_{sh}$. Such a result is expected, since the formally infinite exchange rigidity should lead to a completely coherent rotation of the nanowire magnetization against the background of the magnetic shape anisotropy. According to the Stoner-Wolfarth model, when the field is directed along the easy magnetization axis, equality of the coercive force and the field of this anisotropy should be observed. The decrease of H_c/H_{sh} with increasing of a/l_{ex} is related to the growing role of inhomogeneous magnetization states and, therefore, to a decrease in the instability (nucleation) field with weakening of the exchange interaction [16, 17].

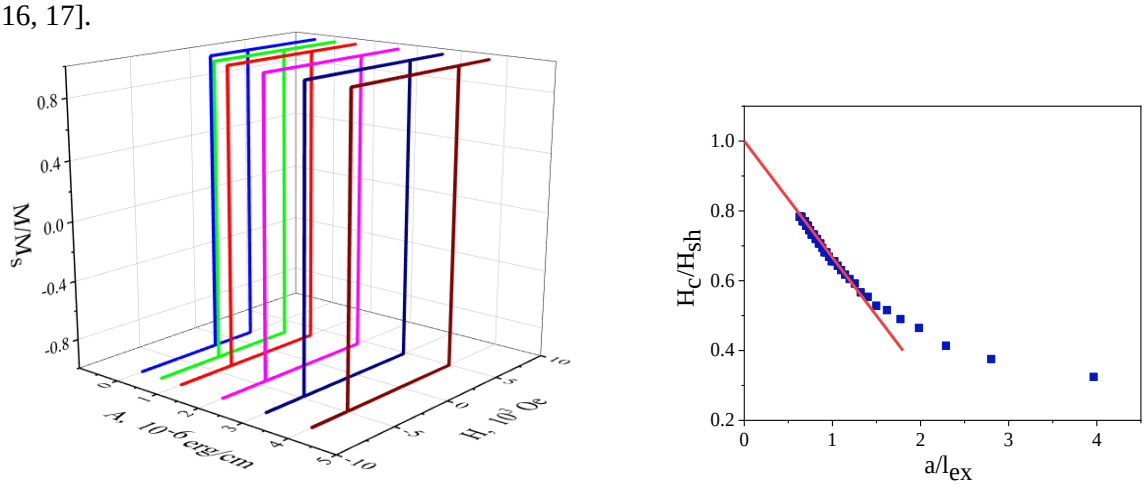

a **b**

Figure 2. a) Hysteresis loops at $K=1.52\cdot10^4 erg/cm^3$. b) Dependence of the coercive force on the exchange constant in reduced units:a/l_{ex} – is the crystallite size normalized to the length of the exchange interaction, H_{sh} - is the shape anisotropy field corresponding to the dipole-dipole interaction. The normalization is the ratio of the contributions from the exchange and dipole-dipole energies. The red line extrapolates the dependence of the normalized H_c to 1, as was predicted by the Stoner-Wolfarth model for large values of A.

*2.3 Series **C**. Normalization problem*

The idea that we have already used and will use further to analyze the numerical results is that the universal regularities in the behavior of the coercive force should be controlled by the ratio of energies that define the micromagnetic problem. We already showed, using the **B** and **D** series as an example, that the energy ratio can be replaced by the ratio of the crystal grain size to the characteristic micromagnetic scale (for series **B** it is l_{ex}, and for series **D** it is δ). For series **C** it is impossible to neglect any of the three contributions to the total energy. Here, neither l_{ex}, nor δ can be considered as a characteristic micromagnetic scale. For this case, we introduce a new scale l_Σ, which is a compromise between the scales used for series **B** and **D**:

$$l_\Sigma = \frac{l_{ex}\delta}{l_{ex}+\delta}. \quad (1)$$

Equation (1) takes into account all energy contributions to the characteristic micromagnetic scale and ensures the correct transition to the limiting cases, considered for series **B** and **D**. As the limiting field taking into account the magnetic shape anisotropy and the crystallite magnetic anisotropy, we take the effective anisotropy field, calculated as: $H_a^{eff} = \sqrt{H_{sh}^2 + H_a^2}$. As a result, in figure 3b we observe the value of H_c/H_a^{eff} passes a maximum at a $a/\delta \approx 3.5 \pm 0.5$. This behavior reflects the correct combination of the limiting regimes of **B** and **D** in a more general situation considering all energy contributions.

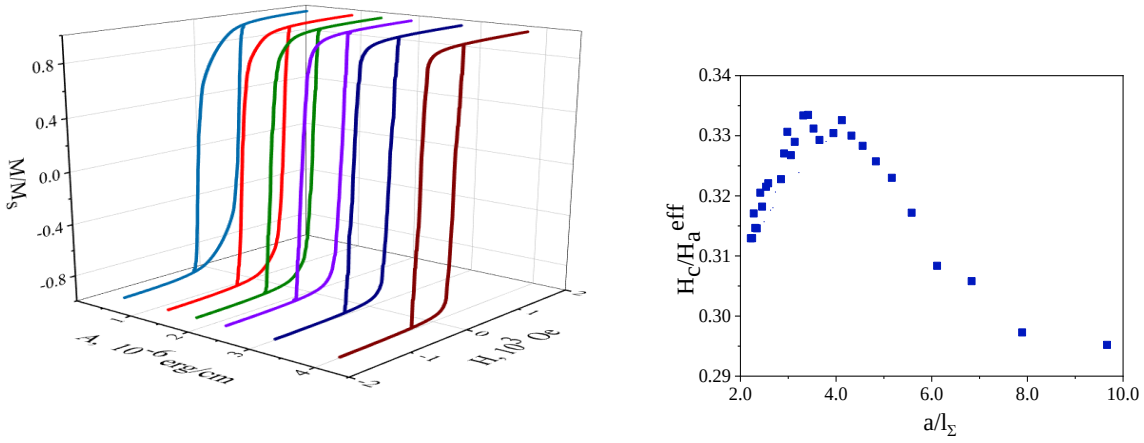

A **b**

Figure 3. a) Hysteresis loops at $K = 3 \cdot 10^6 erg/cm^3$. b**)** Dependence of the coercive force H_c, on the exchange constant, presented in the reduced units. X-axis: ratio of cell size a and averaged length parameter l_Σ. Y-axis: Hc is normalized to the averaged value: H_a^{eff} of the anisotropy field and the shape anisotropy field.

2.4 Series D

Here the main competing contributions are the anisotropy energy and exchange energy. According to table 1, we changed the energy ratio by manipulating the values of the exchange constant. In this case, the ratio of competing energies can also be unambiguously associated with the ratio of spatial scales: $E_a/E_{ex} = (a/\delta)^2$, where the characteristic micromagnetic scale is $\delta = \sqrt{A/K}$ [29,30]. Therefore, we present data on H_c in series **D** in figure 4b depending on the ratio of scales a/δ. The value of H_c here is limited by the magnetic anisotropy field of the crystallite $H_a = 2K/M_S$, therefore, figure 4b shows the reduced coercive force H_c/H_a. According to the RMA model [11,31,32] H_c/H_a should increase, reaching the value of 0.48 at $a/\delta \approx \pi$. Here we see the growth and conditional saturation at $a/\delta \approx 3$. This behavior is in qualitative agreement with the predictions of the RMA model, however, the maximum value to which H_c/H_a tends is still noticeably less than 0.48, predicted

by the Stoner-Wolfarth model. Such a decrease, which is also observed in region III in figure 1b, may be related to the demagnetizing effect of the dipole-dipole interaction, which is excluded from consideration in the Stoner-Wolfarth model.

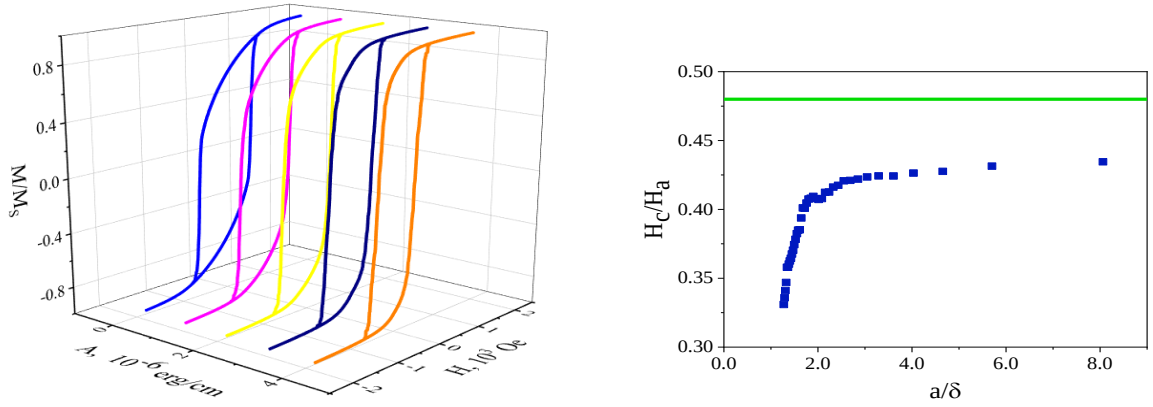

A **b**

Figure 4. a) Hysteresis loops at $K=6.5\cdot10^{6} erg/cm^{3}$. b) Dependence of the coercive force H_c, on the exchange constant, presented in the reduced units. X-axis: ratio of cell size a and length parameter $\delta = \sqrt{A/K}$. Y-axis: H_a - anisotropy field. The normalization is the ratio of the contributions from the exchange energy and the anisotropy energy.

3. Conclusions

Different contributions to the total magnetic energy of polycrystalline nanowires from the exchange, dipole-dipole interaction and magnetic anisotropy of the crystallite can lead to qualitatively different behavior of the coercive force with the crystallite size. Three modes in the magnetic hysteresis behavior were revealed, depending on the ratios of the magnetic anisotropy constant, the exchange and dipole-dipole energies.

In the weak anisotropy mode, when the anisotropy constant is less than the exchange and dipole-dipole energies, its value does not affect the coercive force. With an increase in the crystallite size, a decrease in the coercive force is observed. Here, the behavior of the coercive force is explained by Stoner–Wohlfarth model and the concept of nucleation.

In the strong anisotropy mode, when the anisotropy constant is larger than the exchange and dipole-dipole energies, the coercive force behaves in accordance with the random magnetic anisotropy model, limited by Stoner–Wohlfarth case for extremely large magnetic anisotropy constants of crystallite. It increases with the crystallite size, as well as with an increase of the magnetic anisotropy constant of crystallite. In the limit case of large crystallite anisotropy constants, a readable low level in the coercivity was observed associated with the influence of the dipole-dipole interaction.

In the medium anisotropy mode, when the anisotropy constant is of the same order of magnitude as the energies of exchange and dipole-dipole interactions, a complex nonmonotonic dependence of the coercive force on the crystallite size and the magnetic anisotropy constant is observed. In order to interpret these changes, we propose an equation for the new micromagnetic scale that takes into account all three contributions to the magnetic energy of nanowire, and also performs the correct transition between the limiting cases of weak and strong magnetic anisotropy.

Acknowledgments

This work was supported by the Russian Foundation for Basic Research, Government of Krasnoyarsk Territory, Krasnoyarsk Region Science and Technology Support Fund to the research project 18-42-240006.

References

[1] Sander D *et al*. 2017 The 2017 Magnetism Roadmap *J. Phys. D. Appl. Phys.* **50** 363001
[2] Stamps R L *et al*. 2014 Magnetism Roadmap *J. Phys. D. Appl. Phys.***47** 333001
[3] Fratila R M, Rivera-Fernández S and de la Fuente J M 2015 Shape matters: synthesis and biomedical applications of high aspect ratio magnetic nanomaterials *Nanoscale* **7** 8233–60
[4] Ivanov Y P and Chubykalo-Fesenko O 2015 Micromagnetic simulations of cylindrical magnetic nanowires *Magnetic Nano- and Microwires* (Amsterdam: Woodhead Publishing) pp 423–48
[5] Seng G T and Mansoor B A J 2012 Introduction to the Physics of Nanoelectronics *A volume in Woodhead Publishing Series in Electronic and Optical Materials* (Amsterdam: Elsevier) p 312
[6] Waser R 2012 *Nanoelectronics and Information Technology* (New York: Wiley)
[7] Liu J P, Fullerton E, Gutfleisch O and Sellmyer D J 2009 *Nanoscale Magnetic Materials and Applications* (Heidelberg, London, New York: Springer Science & Business Media)
[8] Mørup S and Hansen M 2007 *Novel Materials. Handbook of Magnetism and Advanced Magnetic Materials* (New York: Wiley) p 3064
[9] Guimarães A P 2017 *Principles of Nanomagnetism* (Cham: Springer International Publishing)
[10] Ivanov Y P and Chubykalo-Fesenko O 2015 Micromagnetic simulations of cylindrical magnetic nanowires *Magnetic Nano- and Microwires* (Amsterdam: Elsevier) pp 423–48
[11] Skomski R 2003 Nanomagnetics *J. Phys. Condens. Matter* **15** R841–96
[12] Ivanov Y P, Vázquez M and Chubykalo-Fesenko O 2013 Magnetic reversal modes in cylindrical nanowires *J. Phys. D. Appl. Phys.* **46** 485001
[13] Ivanov A A, Orlov V A, Patrushev G O and Podol'skii N N 2010 Ground state of the magnetization of nanowires *Phys. Met. Metallogr.* **109** 120–9
[14] Ivanov A A and Orlov V A 2015 Scenarios of magnetization reversal of thin nanowires *Phys. Solid State* **57** 2204–12
[15] Stoner E C and Wohlfarth E P 1948 A mechanism of magnetic hysteresis in heterogeneous alloys *Phil.Trans. Roy. Soc. A.* **240** 559
[16] Aharoni A 1997 Angular dependence of nucleation by curling in a prolate spheroid *J. Appl. Phys.* **82** 1281–7
[17] Aharoni A 1999 Incoherent magnetization reversals in elongated particles *J. Magn. Magn. Mater*. **196**–**197** 786–90
[18] Sellmyer D J, Zheng M and Skomski R 2001 Magnetism of Fe, Co and Ni nanowires in self-assembled arrays *J. Phys. Condens. Matter* **13** R433–60
[19] Nasirpouri F, Peighambari S M, Samardak A S, Ognev A V, Sukovatitsina E V., Modin E B, Chebotkevich L A, Komogortsev S V and Bending S J 2015 Electrodeposited Co93.2P6.8 nanowire arrays with core-shell microstructure and perpendicular magnetic anisotropy *J. Appl. Phys.* **117** 17E715
[20] Yoo E, Samardak A Y, Jeon Y S, Samardak A S, Ognev A V., Komogortsev S V and Kim Y K 2020 Composition-driven crystal structure transformation and magnetic properties of electrodeposited Co–W alloy nanowires *J. Alloys Compd.* **843** 155902
[21] Samardak A S *et al*. 2018 Variation of magnetic anisotropy and temperature-dependent FORC probing of compositionally tuned Co-Ni alloy nanowires *J. Alloys Compd.* **732** 683–93
[22] Samardak A S, Nasirpouri F, Nadi M, Sukovatitsina E V, Ognev A V, Chebotkevich L A and Komogortsev S V 2015 Conversion of magnetic anisotropy in electrodeposited Co–Ni alloy nanowires *J. Magn. Magn. Mater.* **383** 94–9
[23] Komogortsev S V, Chekanova L A, Denisova E A, Bukaemskiy A A, Iskhakov R S and Mel'nikova S V 2019 Macro- and nanoscale magnetic anisotropy of FeNi(P) micropillars in polycarbonate membrane *J. Supercond. Nov. Magn.* **32** 911–6
[24] Komogortsev S V and Iskhakov R S 2005 Magnetization curve and magnetic correlations in a nanochain of ferromagnetic grains with random anisotropy *Phys. Solid State* **47** 495–501
[25] Iskhakov R S, Komogortsev S V, Balaev A D, Okotrub A V, Kudashov A G, Kuznetsov V L

and Butenko Y V 2003 Fe nanowires in carbon nanotubes as an example of a one-dimensional system of exchange-coupled ferromagnetic nanoparticles *J. Exp. Theor. Phys. Lett.* **78** 236–40
[26] Donahue M J and Porter D G 1999 *OOMMF User's Guide, Version 1.0* (Gaithersburg: MD)
[27] Kumar D and Adeyeye A O 2017 Techniques in micromagnetic simulation and analysis *J. Phys. D. Appl. Phys.* **50** 343001
[28] Komogortsev S V, Fel'k V A and Li O A 2019 The magnetic dipole-dipole interaction effect on the magnetic hysteresis at zero temperature in nanoparticles randomly dispersed within a plane *J. Magn. Magn. Mater.* **473** 410–5
[29] Komogortsev S V, Iskhakov R S and Fel'k V A 2019 Fractal dimension effect on the magnetization curves of exchange-coupled clusters of magnetic nanoparticles *J. Exp. Theor. Phys.* **128** 754–60
[30] Komogortsev S V., Fel'k V A, Iskhakov R S and Shadrina G V 2017 Micromagnetism in a planar system with a random magnetic anisotropy and two-dimensional magnetic correlations *J. Exp. Theor. Phys.* **125** 323–32
[31] Herzer G 2013 Modern soft magnets: Amorphous and nanocrystalline materials *Acta Mater.* **61** 718–34
[32] Bolyachkin A S and Komogortsev S V 2018 Power-law behavior of coercivity in nanocrystalline magnetic alloys with grain-size distribution *Scr. Mater.* **152** 55–8